A Quantitative Description of KcsA Gating II: Single-Channel Currents

Sudha Chakrapani,[1] Julio F Cordero-Morales,[1,2] and Eduardo Perozo[1]

[1]Institute of Molecular Pediatrics Science and Department of Biochemistry and Molecular Biology, University of Chicago, Center for Integrative Science, Chicago, IL 60637

[2]Department of Molecular Physiology and Biological Physics, University of Virginia, Charlottesville, VA 22018

The kinetic transitions of proton-activated WT KcsA and the noninactivating E71A mutant were studied at the single-channel level in purified, liposome-reconstituted preparations. Single-channel currents were recorded using patch-clamp techniques under nonstationary and steady-state conditions. Maximum-likelihood analyses reveal that the key influence of acidic pH is to increase the frequency of bursting without an effect on the intraburst open and closed dwell times, consistent with the finding from macroscopic currents that protons promote activation without a significant effect on inactivation. However, in steady-conditions of pH, voltage not only alters the burst frequency but also affects their properties, such as the frequency of the flickers and the dwell times of the closed and open states. This is to be expected if voltage modulates pathways connecting open and inactivated states. Upon opening, KcsA can enter at least two closed states that are not part of the activation pathway. The frequency and duration of these closed states was found to be voltage dependent and therefore these are likely to represent short-lived inactivated states. Single-channel recordings of WT KcsA also show varying propensity for the presence of subconductance states. The probability of occurrence of these states did not show clear modulation by voltage or pH and their origin remains unclear and a focus for further investigation. A kinetic model is proposed to describe the gating events in KcsA that recapitulates its macroscopic and single-channel behavior. The model has been constrained by the single-channel analyses presented in this work along with data from macroscopic currents in the preceding paper.

The Journal of General Physiology

INTRODUCTION

A wealth of structural information on potassium-selective pores has been gathered from KcsA, a proton-activated K^+ channel from *Streptomyces lividians* (Schrempf et al., 1995; Cuello et al., 1998; Doyle et al., 1998; Perozo et al., 1998, 1999; Gross et al., 1999; Liu et al., 2001; Zhou et al., 2001a,b; Zhou and MacKinnon, 2003; Blunck et al., 2006; Cordero-Morales et al., 2006a,b). At basic intracellular pH, the C-terminal half of the second transmembrane (TM) segment of each of the four channel subunits come together as a helix bundle and has been suggested to form a barrier for permeating ions, thereby acting as the primary gate for the channel (lower or activation gate) (Perozo et al., 1999; Liu et al., 2001; Jiang et al., 2002). Several lines of evidence suggest that in response to acidic intracellular pH there are significant conformational changes within the helix bundle that lead to tilting and rotation of the TM segments, which in turn might be related to channel opening (Perozo et al., 1999; Kelly and Gross, 2003). Although the precise location of the pH sensor is still unknown, a recent solution nuclear magnetic resonance (NMR) study has showed that residue H25 at the interface of the two TM segments in the intracellular mouth of the channel changes conformation in a dramatic fashion in response to a change in pH. From this and other observations, the authors implicate this residue as a key component of the pH sensor in KcsA (Takeuchi et al., 2007). However, in the absence of conclusive functional evidences its role as a pH sensor still remains speculative.

Further, upon opening, KcsA shows a time-dependent decay of conductance as the channel enters an inactivated state. EPR measurements showed that the lower gate was open under these conditions (Perozo et al., 1999), suggesting the presence of a second gate (upper gate, inactivation gate) that controls the gating kinetics once the lower gate is open. The transition rate into this state has been shown to be governed by residue Glu71 in the pore helix (Cordero-Morales et al., 2006a). This residue also contributes to the voltage dependence of the inactivation process (Cordero-Morales et al., 2006b). Guided by the knowledge of the underlying regulatory motifs that mediate certain gating reactions, we aim to correlate this structural information with a thorough functional analysis in an effort to provide a framework for physical and mechanistic interpretation of the channel function.

For eukaryotic channels, the first quantitative description of the activation and inactivation gating was provided by Hodgkin and Huxley. They proposed that

Correspondence to Eduardo Perozo: eperozo@uchicago.edu

Abbreviations used in this paper: TM, transmembrane; WT, wild type.

for K^+ channels, gating involved independent transitions of four gating particles such that the rates of these transitions were exponentially dependent on voltage (Hodgkin and Huxley, 1952). This idea was in congruence with the later finding that K^+ channels were composed of four identical subunits with each subunit contributing a voltage sensor toward the activation process (MacKinnon, 1991). Further studies based on more sophisticated patch-clamp measurements of macroscopic ionic and gating currents as well as single channel currents have since suggested that individual subunit transitions during channel activation may not be completely independent and some of these events might be cooperative or even concerted (Bezanilla et al., 1991; Papazian et al., 1991; Stuhmer, 1992; Tytgat and Hess, 1992; McCormack et al., 1994; Smith-Maxwell et al., 1998). Similarly, several other studies have proposed that inactivation process is also not an independent mechanism but is coupled to activation (Goldman and Schauf, 1972; Bezanilla and Armstrong, 1977; Armstrong and Gilly, 1979; Oxford, 1981; Goldman and Kenyon, 1982; Kuo and Bean, 1994). Based on these observations, several tenable kinetic schemes have been proposed that incorporate some level of interactions among subunits during activation and inactivation processes (Bezanilla et al., 1994; Zagotta et al., 1994; Schoppa and Sigworth, 1998b). In all of these models the channel opens only after each of the four subunits has undergone at least one transition between different conformational states. The final step toward channel opening involves a concerted transition. Most models support the idea of a single open state arising from a fully activated closed state. The major point of contention lies in the number of independent and concerted transitions that define the activation pathway. In Kv channels, the independent transitions have been ascribed to the early movements of the individual voltage sensors while the concerted transitions were proposed to involve the coupled motion leading to the opening of the conduction pathway. Although the precise nature of the activating stimulus and consequently the structure of the regulatory domain differ significantly among the members of K^+ channel, they all share a fairly similar topology of the pore domain that harbors the ion permeation pathway. It is therefore reasonable to expect that some of these kinetic events and the associated conformational rearrangements might be conserved among the eukaryotic channels and the 2TM bacterial channels.

In the preceding paper (see Chakrapani et al. on p. 465 of this issue), we analyzed the kinetics of macroscopic currents in detail to understand some of the salient features of activation and inactivation gating of KcsA. We found that like most K^+ channels, KcsA activates with a sigmoidal time course in response to an activating stimulus (pH jump), a feature that has been shown to be associated with the presence of multiple conformational transitions that precede channel opening (Hoshi et al., 1994). The overall time course was found to be appreciably pH dependent and did not show any intrinsic voltage modulation. Upon opening, channels transition into an inactivated state with rates that are generally slower than the rates of activation. These rates are modulated by voltage and by permeant ions with little or no effect by protons. We also found that inactivation can occur from at least one closed state in the activation pathway, and most likely from closed state near the conductive conformation. Furthermore, our results reveal that inactivation entails at least a partial activation of the channel and that the channel can reside in multiple inactivated states depending upon the extent of activation. Recovery from these inactivated states seems to suggest that the different extents of activation might be correlated to differential stability of the inactivated state.

In this paper, we extend our studies to the single-channel properties of KcsA to gain insight into the molecular transitions that underlie the single-channel gating kinetics and how these translate to the overall behavior of macroscopic currents. Measurements were made at different pH and membrane potentials. Transitions among various conformational states were modeled as a time-homogenous Markov process with pH-dependent rates varying linearly with proton concentration and voltage-modulated rates varying exponentially as a function of the membrane voltage. We describe the strategies for the development of a quantitative model to elucidate the activation and inactivation gating in KcsA. The rate constants for several of the gating steps, determined from single-channel and macroscopic currents, were incorporated into the model. This model was then used to simulate the nonstationary and stationary behavior of KcsA.

MATERIALS AND METHODS

Channel Expression and Purification

WT and mutant KcsA were expressed and purified as explained in the accompanying paper and previously published protocols (Cortes and Perozo, 1997). The reconstitution of the channel into the liposomes was done at a low protein to lipid ratio (1:10,000 mass:mass) so as to ensure that there were one to five channels in the patch.

Patch Clamp and Single-Channel Recordings

Single-channel recordings were made in inside-out configurations under both steady-state and nonstationary conditions. Patch pipettes were pulled from thin-walled borosilicate capillaries, coated with Sylgard (Dow Corning Corporation) and fire polished to a final resistance of 2–3 MΩ. Currents were recorded under symmetrical conditions of 200 mM KCl and 10 mM MOPS buffer. pH jump experiments were performed using an RCS-160 fast solution exchanger (Biologic) fed by gravity. During pH pulses, the membrane was held at either ±100 mV. Single-channel currents were recorded using an Axon 200-B patch-clamp amplifier (Axon Instruments, Inc.). The data were digitized at a sampling

rate of 40 kHz and low-pass filtered to 5 kHz through an 8-pole Bessel filter.

Kinetic Analysis

Preprocessing. All kinetic analyses were done using the QuB suite of programs (www.qub.buffalo.edu). Single-channel currents were first inspected visually and sections of data containing erroneous noise and over-lapping channel activity were excluded from further analysis. Drifts in baseline were adjusted using the baseline correction algorithms within the QuB preprocessing module. Current traces were idealized into noise-free open and close transitions using SKM, a segmental k-means algorithm (the Viterbi algorithm) based on hidden Markov modeling procedure at full bandwidth (Qin et al., 1996, 1997), or by a half-amplitude threshold-crossing algorithm after additional low-pass filtering to 2–3 kHz with an incorporated correction for filtering (Colquhoun and Hawkes, 1982). Idealization by SKM yields the relative amplitude, mean duration, and the occupancy probability of the closed and open durations within the record. The closed and open intervals were compiled into histograms with logarithmic abscissa and square root ordinate (Sigworth and Sine, 1987) and were fitted by sums of exponentials of the form

$$f(t) = a_1\lambda_1 e^{-\lambda_1 t} + a_2\lambda_2 e^{-\lambda_2 t} + ...$$

For n states of the same conductance level

$$f(t) = \sum_{i=1}^{n} a_i\lambda_i e^{-\lambda_i t},$$

where a_i is the fractional area occupied by the i^{th} component such that

$$\sum_{i=1}^{n} a_i = 1$$

and λ_i is the reciprocal of the time constant of the i^{th} component.

The number of closed and open states that best describe the data were identified by fitting the data to a linear scheme of closed and open states using a maximum likelihood criteria after imposing a dead time of 25–75 μs.

Isolation of Bursts. A "burst" was defined as a series of openings separated by closed intervals all of which were shorter than a critical duration referred to as the τ_{crit}. The single-channel recordings were idealized and the number of closed and open states determined as described above. τ_{crit} was estimated as the intersection of areas between the second and third closed state durations. This τ_{crit} value was used to isolate burst of openings that arises from one channel activity such that it minimizes the total number of misclassified events (Jackson et al., 1983). Therefore, closed intervals longer than τ_{crit} were considered to correspond to gaps between bursts and those shorter than τ_{crit} belong to closed events within the burst. The τ_{crit} values thus estimated were used to isolate individual bursts within the idealized traces. Only bursts with five or more openings were considered for analysis. The mean duration of open and closed times within the burst were estimated by averaging the corresponding idealized dwell times. These bursts were then categorized based on their mean intraburst open probabilities, which was estimated as intraburst-P_{open} = Mean open time / (Mean open + Mean closed time).

Since quantitative kinetic modeling studies necessitate the selection of kinetically homogeneous population of bursts, only the predominant mode of bursts was chosen for further analysis. Channel activities that did not conform to this population were deleted from the traces. Rate constants were estimated from the dwell-time distributions of the intraburst closed and open intervals using an interval-based maximum likelihood method with an incorporated first order corrections for missed events (25–75 μs) (Horn and Lange, 1983; Roux and Sauve, 1985; Ball and Sansom, 1989; Qin et al., 1996, 1997).

Analysis of Macroscopic Currents. Model-based kinetic analyses of the macroscopic currents were performed using the Mac module within the QuB suite. The rate constants for a given state model and the number of channels in the patch were estimated simultaneously by using a maximum likelihood method (Milescu et al., 2005). The proton binding sites were assumed to be identical and independent, thus reducing the number of free parameters. The rate constants for proton-mediated activation were determined by global fits of recordings made at three different pH values to Scheme 1. The voltage-dependent inactivation rates were assumed to be an exponential function of membrane voltage of the form $\beta(V) = \beta(0)e^{qV/kT}$, where $\beta(0)$ is the forward rate constant at 0 mV, q is the effective charge, k and T denote the Boltzmann constant and temperature in the absolute scale, respectively.

Simulation of Macroscopic and Single-Channel Currents. Stochastic simulations based on Scheme 1 were generated using the SIM module in the QuB software. The parameter values used for simulations were those determined from the macroscopic and single-channel analyses. For pH jump protocols, the leftmost closed state was assigned a unity starting probability assuming that at zero concentration of free proton all the channels exclusively occupy the unprotonated closed state. A sampling interval of 25 and 200 μs were used for single-channel and macroscopic simulations, respectively. The exponential fits and estimation of rate constants for the activation and inactivation phases were done using QuB. Burst analysis of the simulated single-channel data were performed as described above.

RESULTS

Ensemble Average of Single-Channel Currents

Ensemble Average of Single-Channel Currents Were Commensurate with the Macroscopic Properties. To determine whether the macroscopic behavior of KcsA accounts for the activation and inactivation kinetics of channels at the single-molecule level, we performed pH jump experiments for WT and E71A in liposomes reconstituted with few number of channels. Macroscopic current measurements showed that the peak open probability drops close to 30-fold between pH 3.0 and 5.0 (accompanying paper, Chakrapani et al., 2007). As a consequence, for patches that contained only one channel, pH 4.5–5.0 rarely elicited any opening. We therefore, restricted our analysis to measurements from patches with three to five channels.

At each activating pH, the channels are seen to open in a burst of activity before they enter a long-lived nonconductive state (Fig. 1). A burst typically consists of a series of openings and closings in quick successions, flanked on either side by prolonged closures. Steps to more basic pH elicited fewer bursts within each sweep. Across various activating pH conditions, there is also a significant difference in the time delay between the

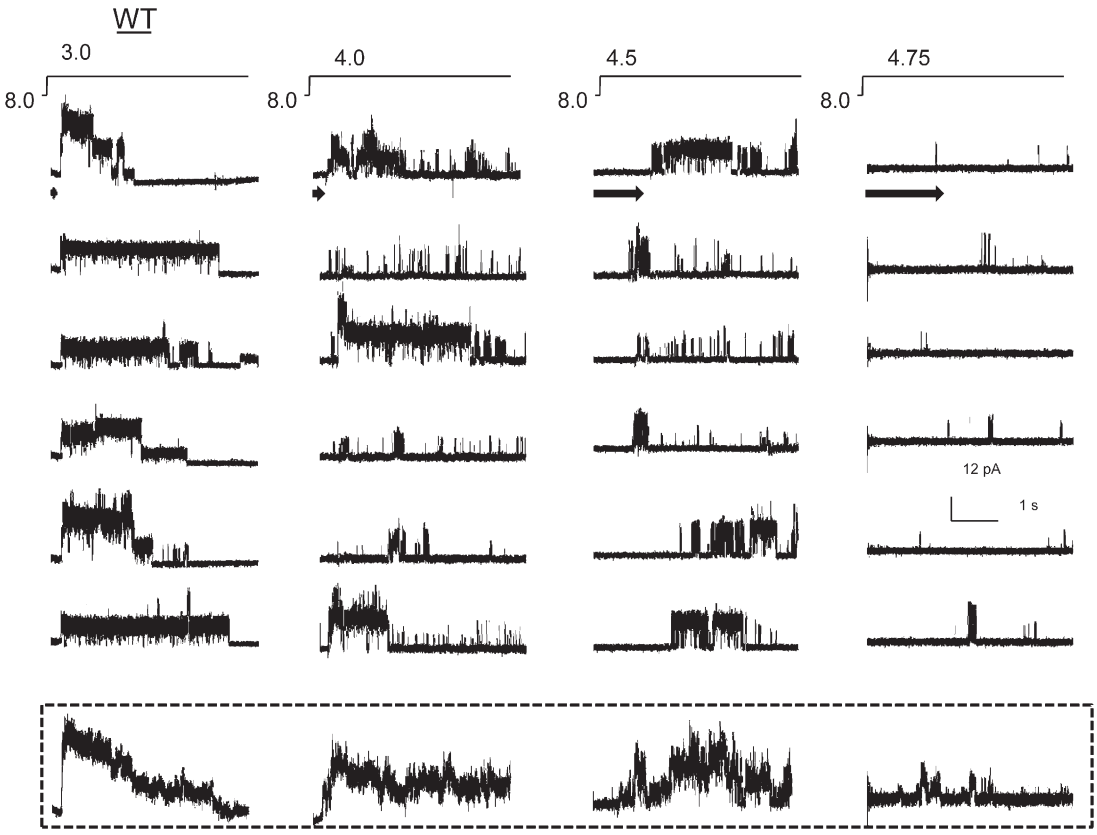

Figure 1. Ensemble average of WT single-channel activity. Inside-out patches from liposomes containing KcsA in a low protein:lipid ratio (1:10,000 mass:mass). Representative openings elicited in response to jumps of indicated pH at +100 mV (top). The arrow marks the delay to first opening. The peak amplitude of current at pH 3.0 reveals approximately three to five channels in the patch. Ensemble averages of single-channel currents from 10 pulses of pH (bottom).

application of the pulse and the first opening (denoted by arrows in Fig. 1). The delay, referred to as the first latency, gets substantially longer at more basic pH. Because differences in first latency are typically reflections of changes in the kinetic mechanism of activation, these finding are consistent with earlier results that show that pH alters the transitions in the activation pathway (Cuello et al., 1998; Heginbotham et al., 1999). The ensemble averages of single-channel currents, obtained by summing 10 sweeps at each pH condition, show that this delay to first opening underlies the sigmoidal rising phase of the macroscopic currents. At more acidic pH, the channel openings appear to cluster close to the start of the pulse and therefore the time course of macroscopic activation occur faster. The time constant for half-maximal activation at pH 3.0 was estimated to be ~20 ms. In contrast, openings in response to pH 4.75, at submaximal activation, are so broadly distributed throughout the sweep and therefore add up to a slowly rising macroscopic current. Upon opening into bursts, the channels enter a fairly long-lived nonconductive state, which is reflected as a decline in ensemble average currents with a time constant of 2.5 s. The values for the activation and inactivation time constant for the ensemble averages are therefore in excellent agreement with the macroscopic rates reported earlier (Chakrapani et al., 2007).

Further, inspection of WT traces shows that even under maximal activation, several pulses (pH 3.0) failed to open all of the channels in the patch. This observation suggests that channels do inactivate before full opening or without ion conduction, a property of KcsA seen in macroscopic two-pulse experiments in the preceding paper and also reported for voltage-gated sodium channels (Aldrich and Stevens, 1983; Aldrich et al., 1983). The occurrence of such events is more obvious in patches with only one channel, where closed-state inactivation is reflected as null traces (unpublished data). This suggests that for WT KcsA, inactivation occurs to a significant extent from states that kinetically precede complete opening and for this reason the measured peak open probability is predicted to be less than 1. Comparable findings have been reported for *Shaker* where the peak open probability has been shown to be close to 0.8 (Hoshi et al., 1994).

Similar studies in the noninactivating E71A mutant (Cordero-Morales et al., 2006a) also showed a qualitative dependency of first latency on pH and the ensemble

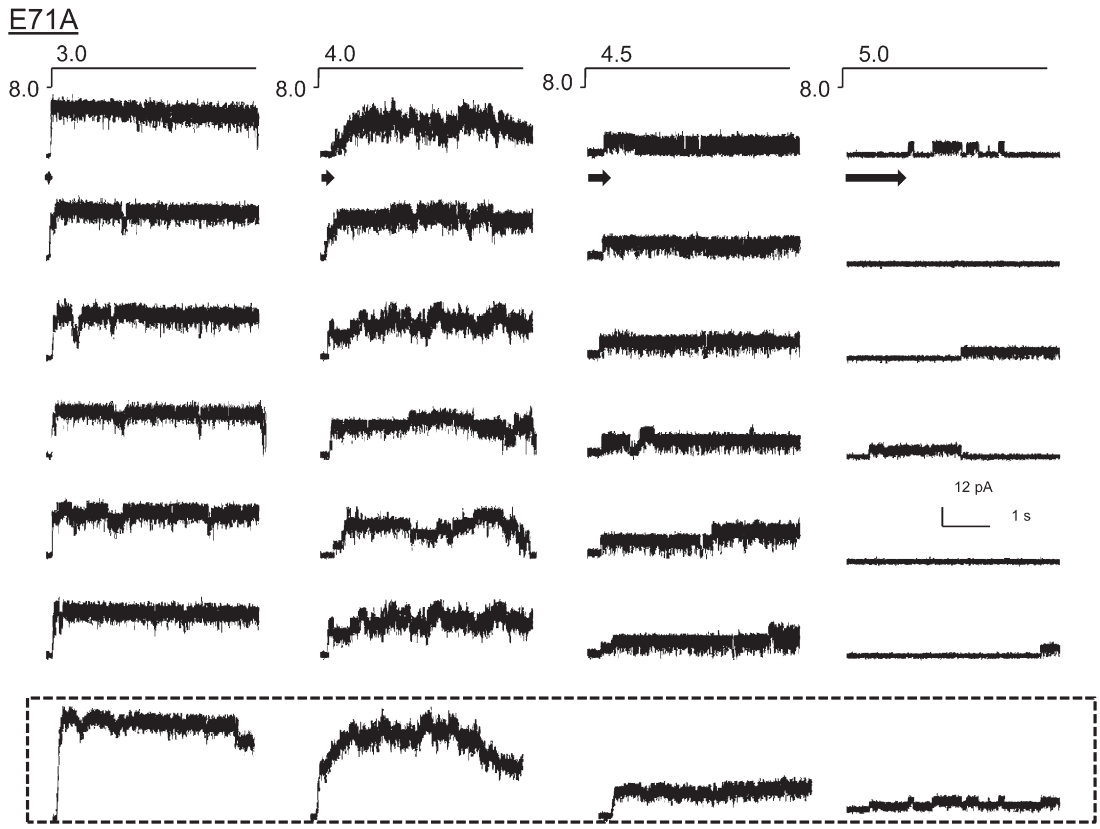

Figure 2. Ensemble average of E71A single-channel activity. Single-channel behavior of E71A, a mutant that removes inactivation, in response to pH jumps (top). Ensemble averages of 10 different pH pulses.

averages reproduced the rising phase of the macroscopic currents (Fig. 2). However unlike WT, E71A mutant channels remained open during the entire length of the pulse and occasionally close briefly into short-lived closed states. The absence of the long-lived closed states is reflected in the ensemble as a nondecaying current. Further, maximal activation (pH 3.0) always elicits the opening of all the channels in the patch, as would be expected for a channel that dramatically slows down inactivation from both open and preopen closed states. Therefore, we consider the peak open probability of E71A to be ~1.0, which is in agreement with the reported steady-state measurement of open probability for single channels. In principle, quantitative evaluation of first latencies requires estimation of the delay to first openings arising from one channel. Due to practical difficulties in recording from patches with just one channel and the inability to quantify delays resulting from the rates of proton buffering and delivery, we have limited our analysis to qualitative comparisons.

Single-Channel Behavior

Kinetic Variability and Modal Gating. At the single-channel level, under stationary conditions KcsA gating is characterized by a highly variable and complex kinetic behavior, the origin of which is poorly understood. The overall gating heterogeneity arises from variation in the open probability as well as mean open and mean closed times (Cordero-Morales et al., 2006a). These parameters vary from patch to patch, even under identical experimental conditions. A careful inspection of steady-state current traces reveals the presence of several different patterns of burst behavior or "modes" (Fig. 3 A). To quantify the behavior of these modes, we chose patches where all types of modes occurred to significant extent. After idealization of current traces using SKM at full bandwidth, bursts of openings were defined using τ_{crit} = 100 ms (see Materials and methods). Bursts with overlapping channel activity were discarded from analysis. A plot of burst P_{open} revealed three distinct populations based on their intraburst open probabilities and flicker kinetics (Fig. 3 B). Representative bursts belonging to each family of modes are shown in left. The "high P_{open}" mode ($P_{open} \sim 0.8$) is characterized by long mean open time and short closed time, while the "low P_{open}" ($P_{open} \sim 0.16$) consists of short openings and long closures. The "flicker" mode ($P_{open} \sim 0.40$) on the other hand is represented by fast gating transitions and short open and closed times. The most predominant mode observed in our experimental conditions corresponds to the "high P_{open}" mode (Fig. 3 A, middle red box), while the "low P_{open}" mode (top red box) and the "flicker" mode (bottom red box) are also

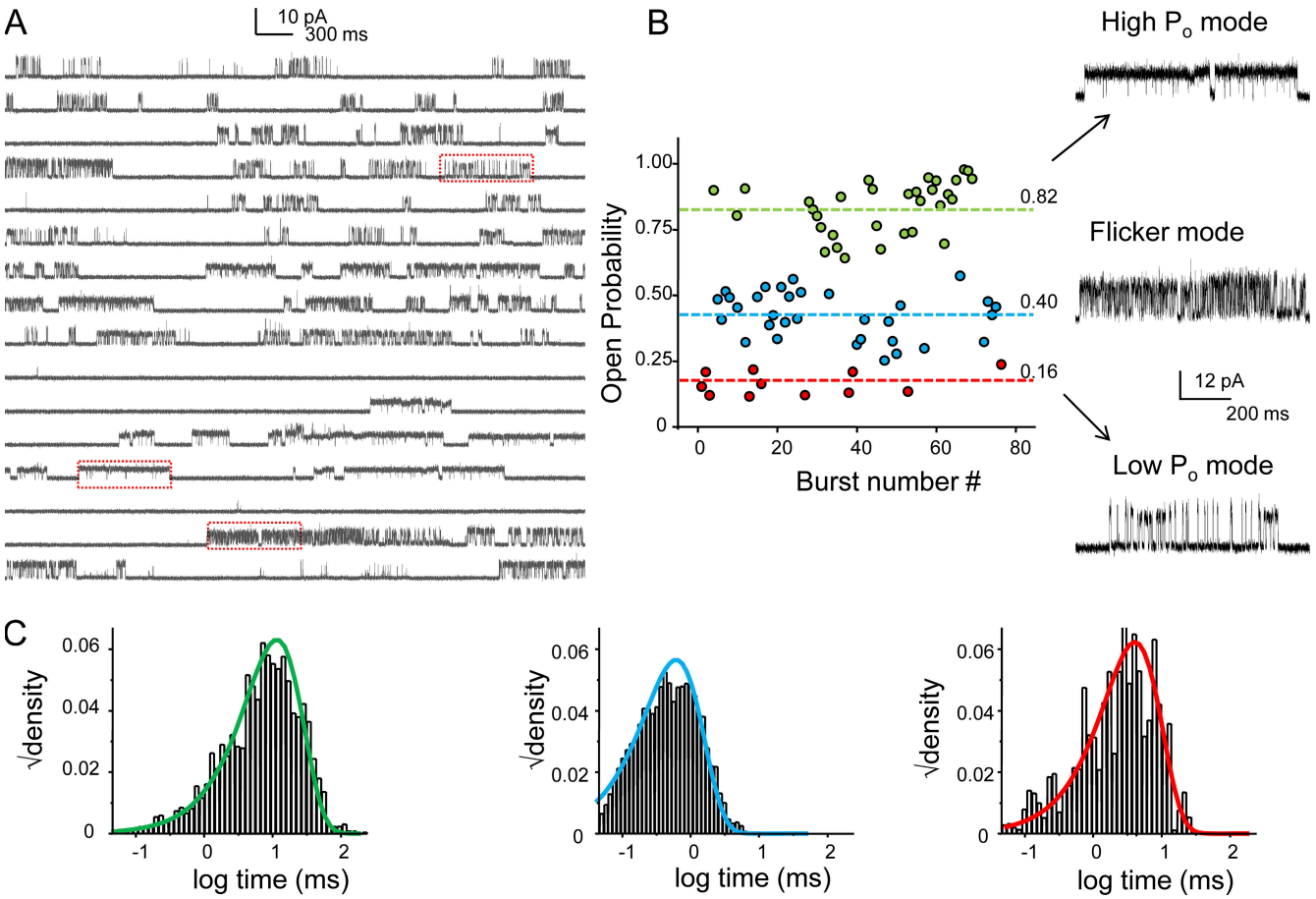

Figure 3. Modal behavior of KcsA. (A) A continuous single-channel recording of KcsA under steady-state conditions at pH 3.0 (maximal activation) with membrane potential at +100 mV. (B) KcsA displays a highly variable kinetic behavior that arises from a combination of three distinct modes of channels activity, the low P_o, high P_o, and the flickery mode. Boxed areas are shown in expanded time scale on the right. The frequency of occurrence of these modes is random and varies from patch to patch. This particular recording was chosen for illustration purpose only to highlight the occurrence of all the three modes. From the distribution of the modes within the trace it can be seen that for this patch the flicker and the high P_o modes seem to be more prevalent, although the occurrence of the flicker mode is rare in most of the patches. (C) The lifetime of the open state within the modes is described by single exponentials.

seen to occur. The plot also reveals that there is no striking time dependence in the distribution of different modes, which suggests that burst modes represent the activity of independent populations of channels. On rare occasions, we observe switching between modes within the same burst, which suggests that the heterogeneity in modal behavior described arises from a homogenous population of channels. Because of this infrequent modal switching and the observation that channels reside predominantly in the inactivated states with an overall low P_{open}, thereby making the determination of the number of channels in patch imprecise, there are no reliable means of determining the rates of switching between modes in the interburst gaps.

Although the open time distribution varied significantly between these modes, the lifetime of the open state within each of these modes was largely confined to a single distribution (Fig. 3 C). The frequency of occurrence of these gating modes varied among patches, a fact that clearly underlies the observed variability in mean open and closed times (Cordero-Morales et al., 2006a). According to these findings, single-channel currents recorded from KcsA incorporated into planar-lipid bilayer appear to gate predominantly in the low P_{open} mode (Heginbotham et al., 1999; Meuser et al., 1999; Splitt et al., 2000; LeMasurier et al., 2001).

Although the variable modal kinetic behavior of WT KcsA is not noticeably modulated by pH or voltage, mutants in the region close to the selectivity filter that either eliminate inactivation (E71A) or dramatically increase the rate of inactivation (Y82A) seem to obliterate this variability to a significant extent (Cordero-Morales et al., 2006a). Therefore it is tempting to speculate that the modal behavior of WT KcsA might result from the intrinsic dynamics of the selectivity filter within a rather flat energy landscape. Note that such heterogeneous kinetic behavior has been reported for a number of voltage- and ligand-gated channel families and with implications in

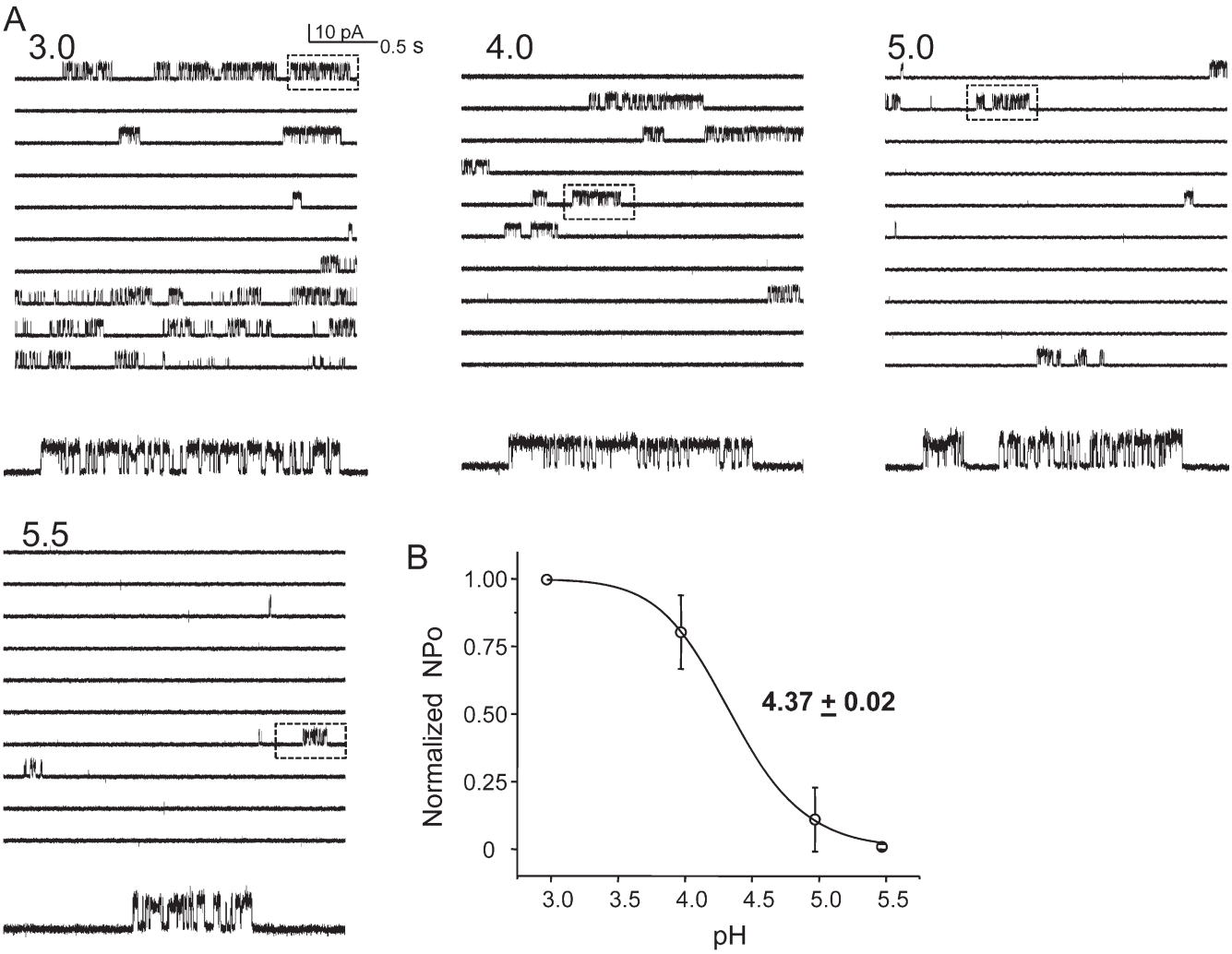

Figure 4. pH-dependent modulation of single-channel behavior of KcsA under steady-state conditions. (A) Representative traces of single-channel currents recorded within the same patch under different pH conditions. Boxed areas denoting burst activity are shown below at higher resolution. Currents were sampled at 40 kHz and low-pass filtered at 5 kHz. (B) The NPo normalized to the value at pH 3.0 (for three patches) plotted against pH and fitted with the Hill equation yields a pKa of 4.37 ± 0.03 and n_H = 1.51 ± 0.06.

their physiological functions (Hess et al., 1984; Auerbach and Lingle, 1986; Patlak et al., 1986; Delcour et al., 1993; Naranjo and Brehm, 1993; Milone et al., 1998; Dreyer et al., 2001).

Another intriguing feature of KcsA gating is the occurrence of subconductance states. These states were reported from early on (Cuello et al., 1998; Meuser et al., 1999; Splitt et al., 2000) and a few recent reports have also disclosed the occurrence of subconductance states in *Shaker* homologues (Chapman et al., 1997; Chapman and VanDongen, 2005). In *Shaker* homologues, the lifetime and frequency of subconductance states were found to be a function of voltage (Chapman et al., 1997; Chapman and VanDongen, 2005). These states were more populated at subthreshold potentials where the overall open probability was low. The openings were proposed to occur when one or more of the subunits transition into the activated position, thereby opening a conduction pathway of intermediate conductance. Along similar lines, we searched for a potential correlation between subthreshold pH and the frequency of occurrence of these states in KcsA. Preliminary analyses reveal a lack of such strict association (unpublished data). Further studies need to be performed to investigate this in greater detail. In this paper we have focused our analyses mainly on the effects of pH and voltage on the most prevalent gating mode (high P_{open}) and on the properties of only the full-conductance state.

Modulation of Gating Kinetics by pH

Increases in the NP_{open} Arise from Increase in Frequency of the Bursts without a Change in the Burst Behavior. Single-channel currents of KcsA recorded in bilayer systems under steady-state conditions have shown that acidic pH increases the NP_{open} (Cuello et al., 1998; Heginbotham et al., 1999; Meuser et al., 1999). Since under steady-state

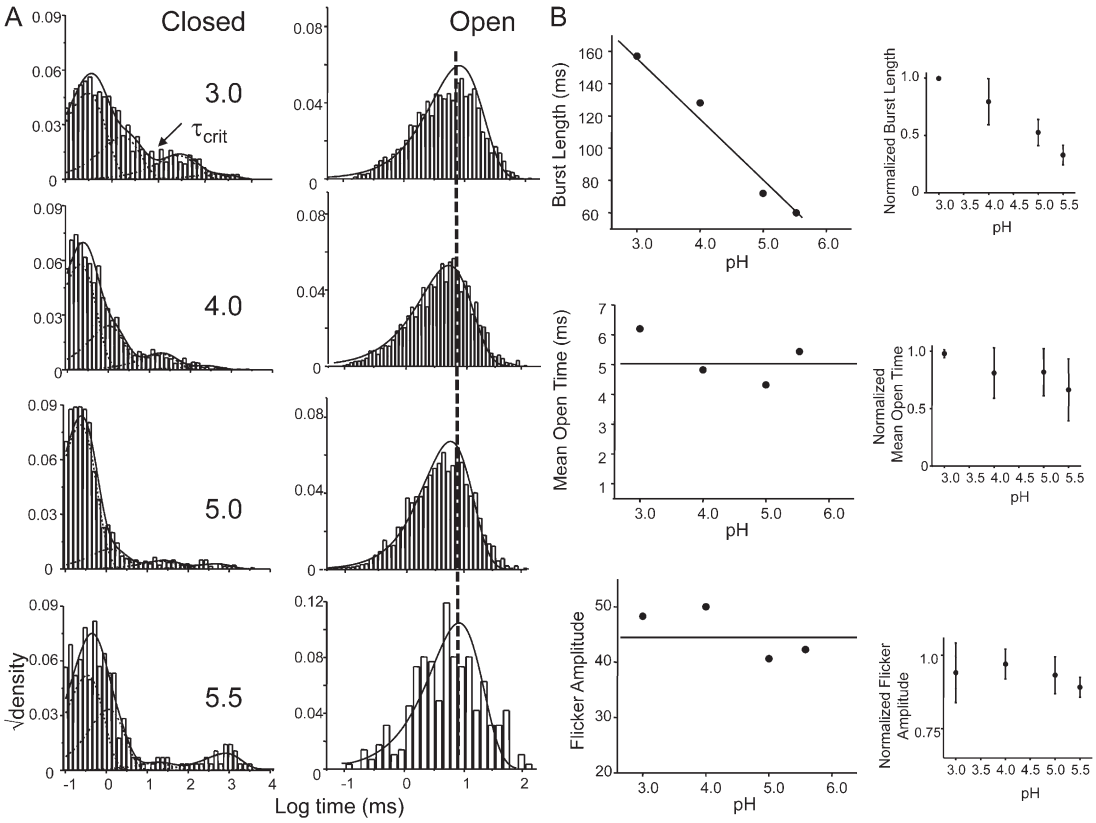

Figure 5. pH increases the frequency of channel activity without an effect on the burst behavior. (A) Closed and open interval dwell-time distributions for the entire record and the smooth line corresponds to the density functions calculated from the optimal fit using a four closed and one open state model. (B) Kinetic analysis after extracting bursts of channel activity by using a critical time (τ_{crit}). The "burst" consisted of the open state and the two shortest closed states, which most likely comes from a single-channel activity. (Inset) Normalized values for six patches.

conditions, KcsA channels predominantly populate the inactivated state, the observed increase in NP_{open} is not necessarily a manifestation of activation but is also of the recovery from inactivation. Therefore, the effect of pH on open probability could arise from a combination of these two pathways. Our macroscopic measurements under nonstationary conditions show that the effect of pH in increasing the open probability comes mainly from favoring transitions from the closed state(s) toward the open state, without a concomitant change in the transition rate toward the inactivated state (Chakrapani et al., 2007). In principle, an increase in peak open probability can also arise from parallel contributions from increase in mean open time, burst length, and duration of bursts. To address these possible contributions, we measured single-channel currents, from typically 15–20-min recordings, under stationary conditions between pH 3.0 and 5.5 (the range of pH within which most of our macroscopic current measurements were made). Fig. 4 A shows representative single-channel currents at +100 mV at increasing pH values. Under steady-state conditions, the majority of the channels reside in the inactivated state, punctuated by brief periods of recovery observed as bursts of openings (Fig. 4 A).

The open probability within the patch, NP_{open}, increases ~30-fold between pH 5.5 and 3.0, in close agreement with measurements from macroscopic currents (Fig. 4 B) (Chakrapani et al., 2007). The closed and open duration elicited by pH pulses were analyzed in the framework of a time-homogenous Markov process (Qin et al., 1997). The dwell times, at all pH conditions, were fitted with the maximum likelihood estimates of distribution containing one open and four closed states in a linear (C-C-C-C-O) scheme (Fig. 5 A). Decreasing pH promotes a dramatic shortening of the lifetimes of the longest closed state (~20-fold between pH 5.5 and 3.0). This closed state represents the gaps between bursts and it is therefore the key determinant of the steady-state P_{open}. While at full activation (when the pH-sensitive lower gate is completely open), the long closures are dominated by the long-lived inactivated states, under conditions of subthreshold activation these states reflect closures both within the activation and inactivation pathway. The open channel dwell time is described by a single-exponential distribution and displays little or no dependence on pH. The predominant effect of increasingly acidic pH appears to be to increase the frequency of openings.

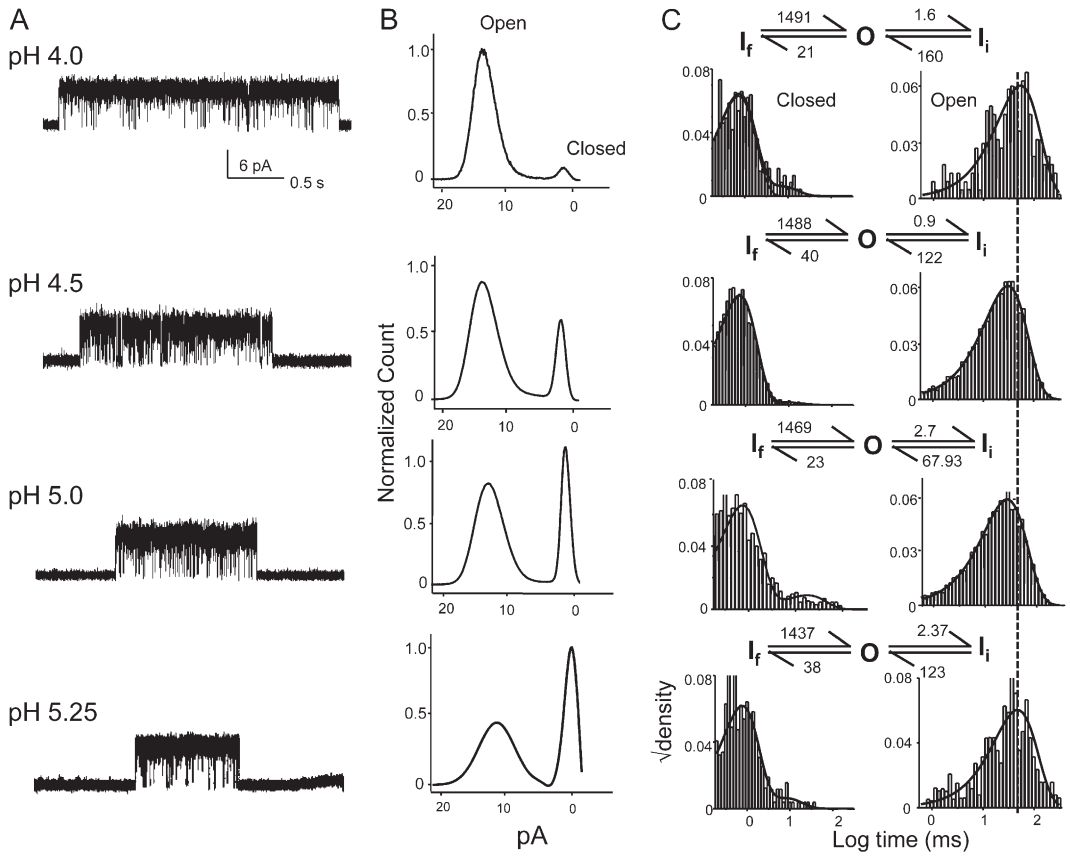

Figure 6. Burst properties of E71A are not modulated by pH. (A) Representative single-channel traces displaying burst activity at various pH. (B) Amplitude histogram for the entire record shows the effect of pH in decreasing the lifetime of the closed state without an effect on the conductance of the open state. (C) Distribution of open and closed interval within bursts isolated using τ_{crit}. The superimposed density functions were calculated by fits to model shown above the histogram. The rate constants are s^{-1}.

We then isolated bursts that correspond to a single-channel activity by choosing an appropriate τ_{crit} as described in the Materials and methods (Fig. 5 B). The burst comprised of the two shortest closed states and the open state. The results of analysis of these bursts are shown in Fig. 5 B. The burst duration was found to increase 2.5-fold between pH 3.0 and 5.5, while the mean open time did not change significantly within the pH range. The fast component in closed-channel dwell time distribution corresponds to the fast flicker states (denoted by I_f) and is the predominant closed event in the single-channel record. The duration ($\sim$0.2–0.5 ms) and the frequency of occurrence of this closed state were found to be invariant with pH. The second component of the closed duration distribution (I_i, intermediate closed state) has a lifetime of 2–5 ms and is also pH insensitive.

We then studied the effect of pH on the gating behavior of the channel in the absence of inactivation (E71A mutant). Fig. 6 shows representative current traces of E71A at different pH and their corresponding amplitude histograms. At acidic pH (4.0), the channel showed an $NP_{open} \sim 1$, while at more basic pH (5.0) the channels opened into short burst of openings and entered into fairly long closures. The occurrence of these long-lived closed changed with pH. Since macroscopic currents elicited from E71A do not show inactivation in this pH range, the long duration closures most likely constitutes the closed states in the activation pathway. The events within the bursts at different pH were best fit by a kinetic scheme consisting of two closed states and one open state, which again represents a subset of the overall gating behavior of the channel and consists only of the states that the channel enters after opening at acidic pH. The lifetime or the frequency of the shortest dwell time closed state (I_f, flicker state) and the intermediate closed state (I_i) are not affected by pH and therefore could represent a short-lived inactivated state from which the channel recovers quickly. As in WT KcsA, the distribution of the open duration within these bursts displays very little dependence on pH.

Together these results from WT and E71A suggest that once the channel opens. pH does not modulate the rates that govern transitions between various conformational states that are involved in inactivation gating. Since the distribution of open channel dwell time does not vary significantly with pH, whereas the first latency appears to vary appreciably, we conclude that the pH dependency of macroscopic kinetics arises mostly from

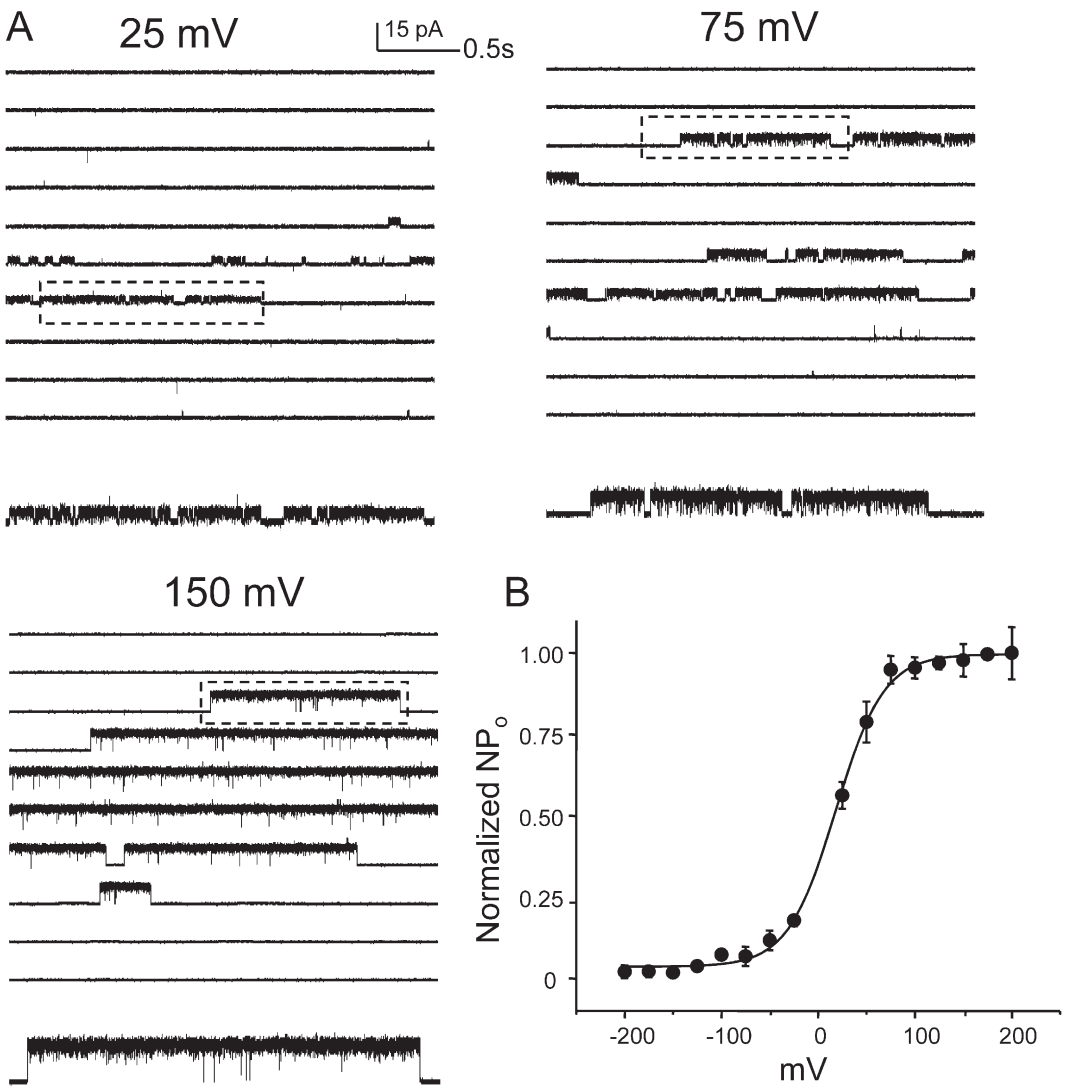

Figure 7. Steady-state behavior of WT KcsA is modulated by voltage. (A) Single-channel currents recorded at pH 3.0 under different membrane potentials. Boxed regions are shown in high resolution below. (B) A plot of NP_{open} vs. voltage (from five patches) shows the modulation of steady-state open probability by voltage.

steps leading to the open state rather than from the open state itself. Further, the distribution of the mean open time (10–100 ms) is much shorter than the decay time constant of the macroscopic current (1–3 s). As in the case of channels that reopen several times before inactivating, the inactivation time constant of KcsA is a reflection of the burst length (0.1–1 s) rather than the mean open time (Wyllie et al., 1998).

Modulation of Gating Kinetics by Voltage

Increases in the NP_{open} Arises from Increase in the Frequency and Duration of the Burst. The modulation of steady-state open probability of WT KcsA by voltage has been reported by several studies (Cuello et al., 1998; Heginbotham et al., 1999; LeMasurier et al., 2001; Cordero-Morales et al., 2006b). With recent evidences it is becoming increasingly clear that the molecular basis of this modulation comes from the voltage dependence of the inactivation process (Cordero-Morales et al., 2006b). KcsA displays two types of voltage-dependent asymmetries, inactivation and open channel noise (Cuello et al., 1998; Heginbotham et al., 1999). Inactivation rates, as measured from the time constant of macroscopic current decay, change 10–15-fold between ±150 mV. The I-V plots show that at depolarizing potentials, KcsA shows rectification of outward current, while at hyperpolarizing potentials, there is a noticeable decline in the current amplitude along with high incidence of short-lived flickers (Heginbotham et al., 1999). To understand the microscopic gating events modulated by voltage we analyzed the single-channel behavior at different membrane voltages. Fig. 7 shows representative current traces recorded under steady-state conditions of pH 3.0 at indicated membrane potential. A plot of

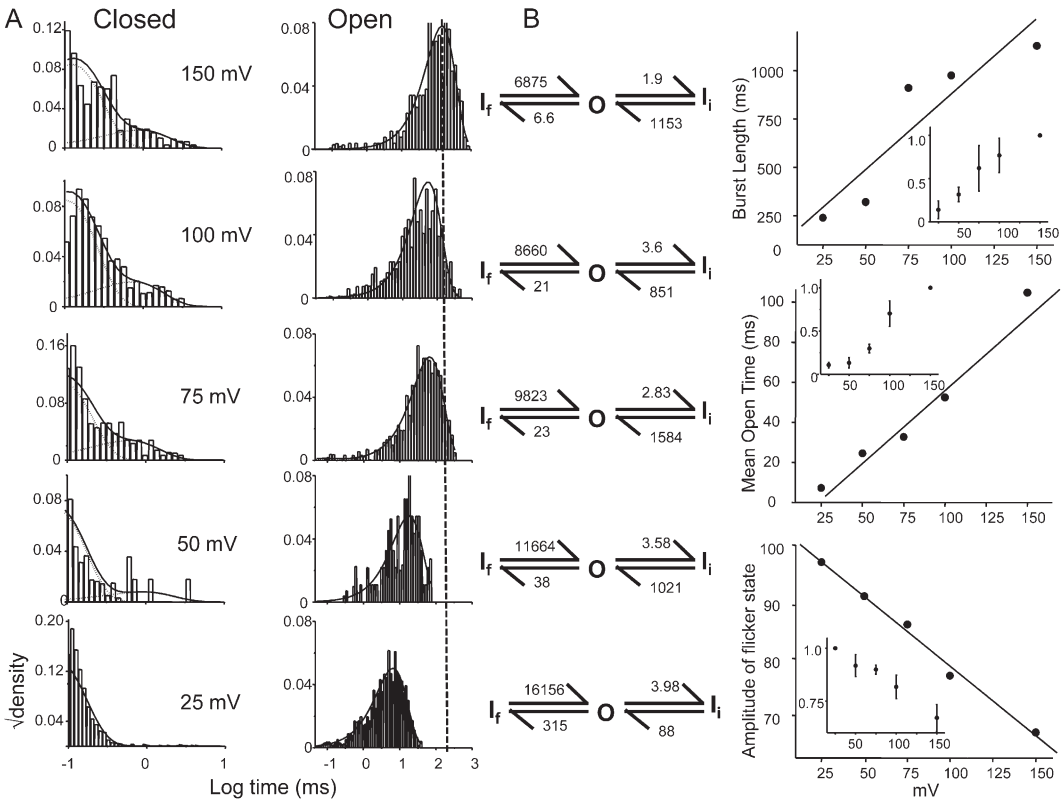

Figure 8. Voltage modulates the frequency and the behavior of bursts. (A) Dwell time distribution of closed and open events within bursts identified using τ_{crit}. Idealization and analysis of the burst were done at full bandwidth (40 kHz acquisition and 5 kHz filter) using SKM in the QuB suite. The solid line denotes the density function calculated by fitting to two closed and one open state model. (B) The properties of the burst as a function of voltage. (Inset) Normalized values for three patches.

NP_{open} as a function of membrane potential is well fit as a Boltzmann distribution with a midpoint at +10 mV and a z value of 0.7 e_o (Fig. 7 B). Since at hyperpolarizing membrane potential the amplitude of the currents was small and the open channel noise very high, we limited our analysis to the data in the range of +25 to +150 mV. The increase in open probability was brought about by a decrease in the long closures corresponding to gaps between bursts of channel activity. An increase in the lifetime of the longest closed state (inactivated state, I_s) with more negative potentials suggests that the rate of recovery from inactivation is significantly slower at these potentials. Fig. 8 A shows the burst duration histogram (left) overlapped with the density function obtained from an optimal fit to a scheme of two closed and one open state (right). Fig. 8 B shows that the length of the burst increases by approximately five times between +25 and +150 mV. This increase in the length of the bursts arises predominantly from increases in the lifetime of the open state, which increases ~10 fold. The lifetimes of the two closed states are also modulated by voltage as revealed by the rate constants in Fig. 8 B. The most prominent effect being an increase in the frequency of the flicker state (I_f) along with a decrease in their lifetimes at more negative potentials (Fig. 8 A). The dwell time of the open state is described as the inverse of the sum of all the exit rate constants from the open state and this value is dominated by rate constant connecting the open state to the shortest closed state (in this case, it corresponds to the flicker state). These flicker states are more prevalent at hyperpolarized potentials, resulting in an overall decrease in channel open lifetime. One potential candidate giving rise to flickers could be the side chain of residue Glu71, which governs the voltage dependence of the slowest inactivation rate. Although neutralizing this charge (E71A) does not completely eliminate this flicker state, it does reduce the voltage dependence of the transitions to and from the flicker to a large extent (unpublished data). The second possibility is that flicker could arise from an open channel block by ions in solution. The frequency of flicker transitions increases considerably at hyperpolarized potential, a phenomenon that could be explained if blocking ions significantly enter the membrane electric field. The lifetime of the intermediate closed state (I_i) tends to get longer with hyperpolarization (similar to I_s), suggesting that this state might represent a short-lived (nonabsorbing) inactivated state. Further, the occurrence of two short-lived closed states (~0.3 and ~5 ms) that are not part of

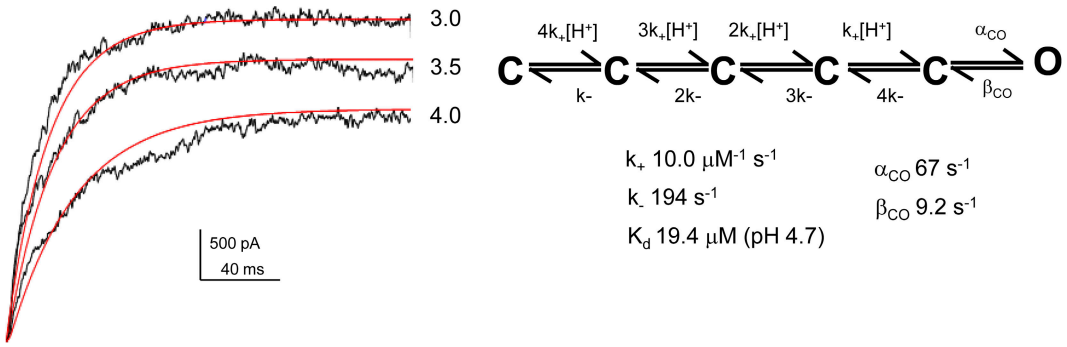

Figure 9. Global fitting of macroscopic current responses using maximum likelihood-based method to estimate the rate constant in the activation pathway. The rising phase of the macroscopic activation recorded at pH 3.0, 3.5, and 4.0 was simultaneously fit to the scheme (right) to get a direct estimate for the on and off rate for proton binding and the channel opening and closing rate constants. The scheme was constrained to assume that proton binding to all the subunits is equal and independent.

the activation pathway has been reported for *Shaker*, although these states have been found to be nearly voltage independent (Hoshi et al., 1994; Schoppa and Sigworth, 1998a).

We therefore conclude that hyperpolarizing potentials decrease the frequency of bursts as well as shorten their duration thereby causing dramatic effects on open probability. The decrease in burst lengths occurs as a consequence of the voltage-enhanced rate of entry into the long-lived inactivated state, while the decrease in the mean open time arises from an increase in the rate of the flicker state. Together they lead to voltage-modulated decline of macroscopic conduction as seen under nonstationary conditions (Chakrapani et al., 2007).

Strategy for Model Development. In this and the accompanying paper we characterize several features of the activation and inactivation gating of WT KcsA and a noninactivating mutant E71A under single-channel and ensemble conditions. These data will be used in the following section to derive a quantitative model for KcsA gating and obtain direct estimates of the rate constants for some of these gating events. Our scheme assumes a time-homogenous Markov model for gating in which transitions occur among discrete conductive and nonconductive states (Fig. 8).

(SCHEME 1)

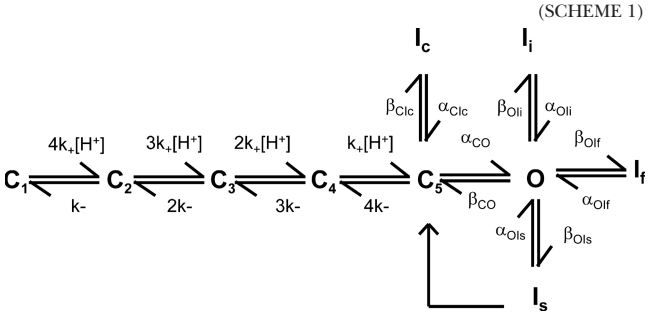

In this scheme, activation of KcsA is described by sequential transitions among five closed states before channel opening. The fast rising phase of the macroscopic current is always proceeded by a delay or foot that becomes more prominent at basic pH (Chakrapani et al., 2007), a result that suggests the presence of multiple closed states in the activation pathway. However, given the uncertainty in the number of closed states that can be fit to the foot of the rising phase of the macroscopic and considering the tetrameric organization of identical subunits in KcsA, we choose to use four closed states, each corresponding to different number of protons bound. Although fitting pH-dependent activation of KcsA with the Hill equation yields a value of ~1.8–2.0, suggesting some degree of cooperativity in the activation pathway, as a first approximation we will assume that the binding of protons to each of the four subunits is an equal and independent event. We incorporated a pH-independent final transition from the fully protonated closed state to the open state to account for the similarity in the bursting behavior of the channel at different pH conditions (Fig. 5). Such schemes with a combination of independent and concerted gating transitions have been successfully used to account for macroscopic currents, gating currents, and single channel data for *Shaker* and voltage-gated sodium channels (Armstrong and Gilly, 1979; Vandenberg and Bezanilla, 1991; Tytgat and Hess, 1992; Bezanilla et al., 1994; McCormack et al., 1994; Zagotta et al., 1994; Schoppa and Sigworth, 1998b).

Our model describes ion conduction to occur from a single open state. The highly variable modal kinetic behavior of KcsA is not taken into consideration in the present scheme. KcsA has an extremely low spontaneous activity (at pH 8.0), suggesting that the opening of the channel from the unprotonated closed state is a relatively rare event. Further, since the predominant component of the open time distribution and the behavior of the burst does not change with pH (even though the open probability changes dramatically), we reason that the channel only opens from one closed state (most likely from the fully protonated closed state). We therefore

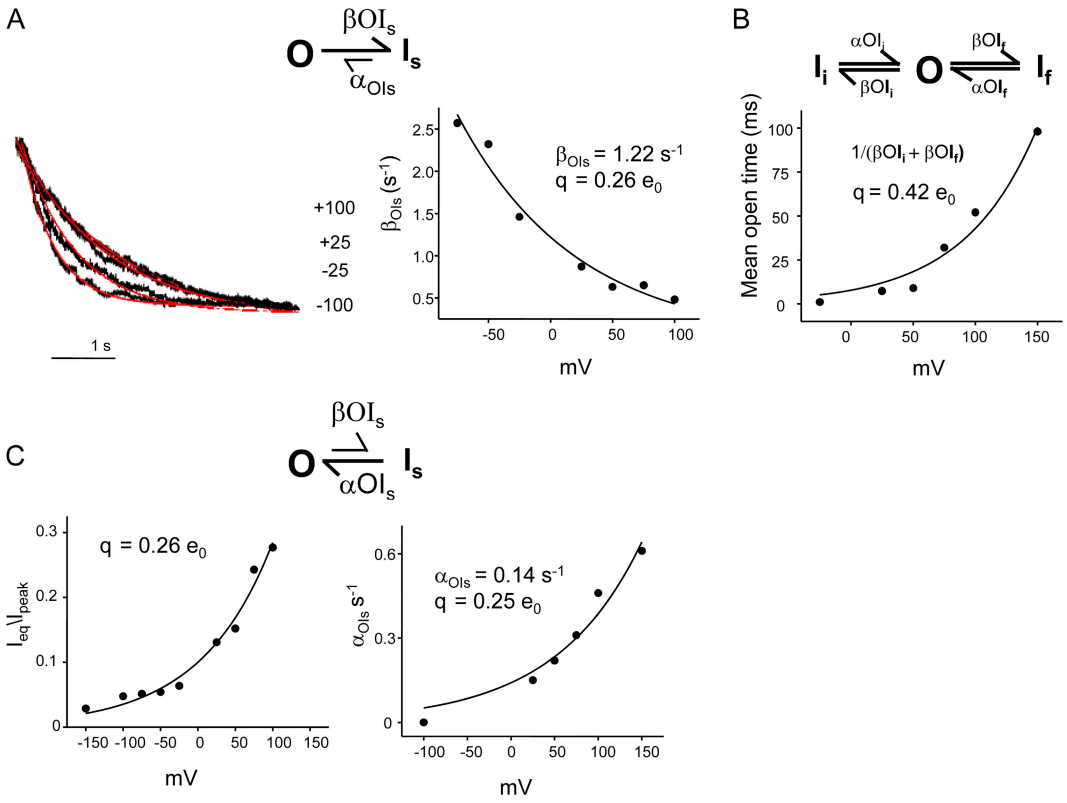

Figure 10. Estimation of the rate constants and their voltage dependencies in the inactivation pathway. (A) The decay time courses of the macroscopic currents elicited by jumps to pH 3.0 at different membrane potentials were fit to Scheme 1. The βOI_s estimated from the scheme was plotted as a function of voltage and fit using the equation $\beta(V) = \beta(0)e^{q\psi/kT}$, yielding βOI_s (0) = 1.22 s^{-1} and q = 0.26 e_0. (B) To estimate the voltage dependency of the two short-lived closed states within the burst, the mean open time derived from single-channel analysis was fitted as an exponential function of voltage, which yields a partial charge of q = 0.42 e_0. (C) Steady-state recovery from inactivation was estimated from the macroscopic records as ratio of steady-state current to its peak value (left). Steady-state recovery is also reflected in the lifetime of the longest closed state in the single-channel currents under equilibrium conditions (right). Both measurements reveal a partial charge of q = 0. 25 e_0 with this conformational change.

believe that in WT KcsA, ion conduction does not occur until all of the subunits are in the open conformation and, therefore, the ion conduction most likely occurs through a concerted conformational change of all of the four subunits (Chakrapani et al., 2007).

Once open, KcsA enters into a nonconducting, inactivated conformation (I_s) from which the channel shows a very small rate of recovery accounting for ~5–10% of the peak current at steady state (at depolarized potentials). Prepulse experiments show that KcsA inactivates also from closed state(s) before channel opening (I_c), an indication that full channel opening and ion conduction is not a prerequisite for deep inactivation to occur (Chakrapani et al., 2007). In our model, the recovery from inactivation occurs from pathways connecting inactivated states to the closed states without passing through the open conductive states, as seen from monoexponential decay kinetics and lack of repriming currents during deactivation. Stationary single-channel kinetic analysis reveals the presence of at least two closed states within a burst of channel activity. The lifetimes of these states are unaffected by pH but are modulated by voltage. Given these properties, we suggest that these states correspond to short-lived inactivated states that are not part of the activation pathway. In our kinetic scheme these are represented as I_f (flicker closures) and I_i (intermediate closures).

To derive rate constants for various transitions that constitute the activation and inactivation gating of KcsA, we used a combination of macroscopic and single-channel measurements, recorded under different conditions of pH and voltage.

Estimation of Rate Constants in the Kinetic Scheme. Macroscopic currents were analyzed using a maximum likelihood method incorporated in Mac module of the QUB software. The forward and reverse rate constants for channel activation were determined by global fits of the activation time courses at pH 3.0, 3.5, and 4.0 to the five closed state–one open state kinetic scheme (Fig. 9). The model was constrained in accordance with the assumption that proton binding to the four subunits is identical and independent. The results of the fit gave us a K_d of

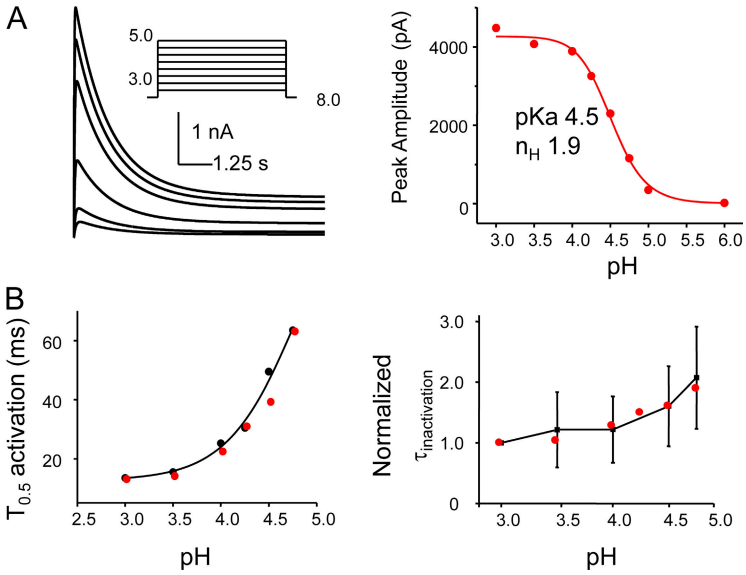

Figure 11. Model-based simulation of macroscopic currents. (A) Simulation of macroscopic currents in response to pH jumps using Scheme 1. Dose–response curves fitted with Hill equation yields a pKa of 4.5 and the Hill coefficient 2. (B) pH dependence of the half-maximal activation and inactivation time constants. The black and red circles represent the experimental and simulated values, respectively.

19.4 μM (pH 4.7) for proton binding. This value is in close agreement to the pKa estimated from the peak of the macroscopic response (pH 4.2) and from the single-channel steady-state measurement (pH 4.3).

Once open, the channel displays at least three kinetically distinct nonconductive states (I_s, I_i, and I_f). The estimates for the rate of entry into I_s and its voltage dependence was obtained from the monoexponential kinetics of macroscopic decay elicited by pH 3.0 at different membrane potentials. The time course of current from the peak of maximal activation to the steady-state value is primarily governed by the entry rate into the slowest component of the inactivation. A fit to the OI scheme yields an estimate of the forward transition into I_s, βOI_s (Fig. 10). Estimate of the charge q that determines the voltage sensitivity of β_{OIs} was obtained by fitting an exponential function (Materials and methods) to βOI_s between −75 and +100 mV, where the $\beta OI_s >> \alpha OI_s$. The fit gives a value of $\beta(0) = 1.22\ s^{-1}$ and $q = 0.26\ e_0$ (Fig. 10). The rate constants for the two inactivated states (I_f and I_s) were estimated from single-channel bursts analysis as shown above in Fig. 8. The voltage dependence of these states, determined by fitting the mean open time (which is an inverse of the sum of βOI_i and βOI_f) as an exponential function of the voltage yields a q of 0.42 e_0. Together, the three forward transitions from the open state into the inactivated states are associated with an equivalent of 0.68 e_0.

To get an estimate for the partial charge involved in the recovery from slow inactivation (I_s), we used both macroscopic and single-channel measurements. In macroscopic currents, recovery from inactivation was measured as the ratio of the amplitude of the steady-state current to its peak value and when fitted to an exponential function of voltage yielded a value of 0.26 e_0. In the single-channel record, this rate is a measure of the reciprocal of the lifetime of the longest closed state. Although, this value is directly affected by the number of channels in the patch, it nevertheless yields an approximate estimate of the charge associated with this gating process. If we assume there were approximately three to five channels in the patch (which is a reasonable approximation under these conditions), the value for $\alpha OI_s(0) = 0.035\ s^{-1}$ and $q = 0.25\ e_0$. Further, as shown in Fig. 8, the rate constant for the recovery from the I_f and I_i also show a residual voltage sensitivity (approximately twofold change between +150 and +25 mV). Even though we have not assigned an associated charge with the voltage dependence of the recovery of the channel from I_s, upon closure of the lower gate, recovery measurements reveal an approximately threefold change between +100 and −100 mV (Chakrapani et al., 2007). Further, closed-state inactivation also appears to involve an associated charge movement that needs to be quantified. Since these rates were approximately sixfold slower and the recovery appeared to be at least twofold faster than open state inactivation, we incorporated the approximate rates into the model. Together these voltage dependencies reflect the q of 0.72 e_0 measured from the distribution of NP_{open} at different voltages as shown previously (Cordero-Morales et al., 2006b).

Model-based Simulation of KcsA Gating. To test the predictions of our kinetic model, we simulated macroscopic and single-channel currents using the SIM module of QuB software and estimated the kinetic parameters. Fig. 11 A shows the macroscopic activation in response to pH jump and the corresponding dose–response curve. The simulated traces depict the fast rising phase of the macroscopic followed by a slow decay to the steady-state value. A fit of the Hill equation yields a pKa of 4.5 and Hill coefficient of 1.9. These values are in excellent agreement with those estimated from the experimental measurements. A comparison of the time constant for

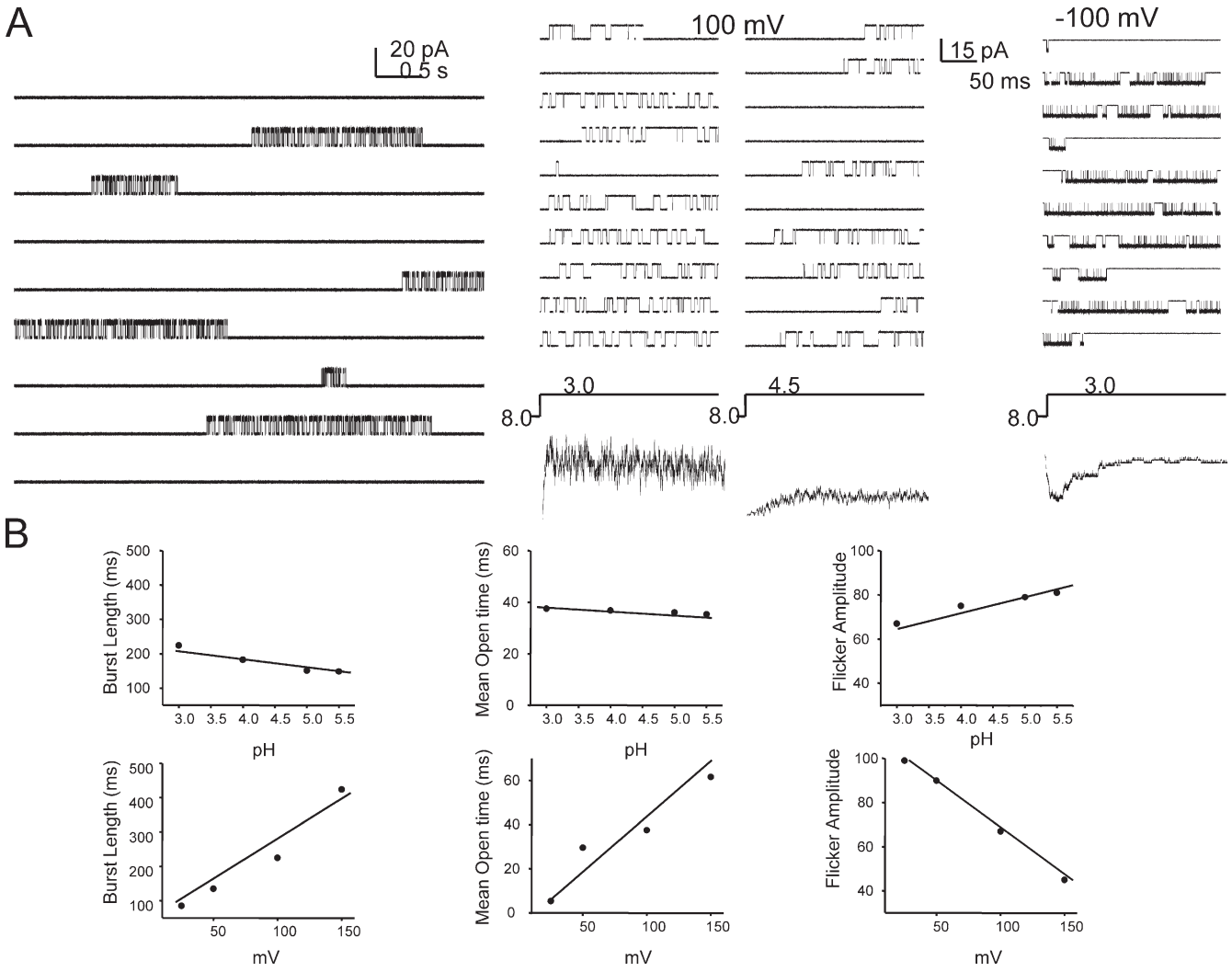

Figure 12. Model-based simulation of single-channel currents. (A) Stationary (left) and nonstationary (right) properties of single-channel currents based on Scheme 1. (B) Kinetic properties of the burst at various conditions of pH and membrane voltage.

half-maximal activation and inactivation ($T_{0.5}$) estimated from the simulated currents (red) with those determined experimentally (black) shows the pH sensitivity of the rise time of activation and a relatively weak pH dependency of the inactivation rates, as seen experimentally.

Single-channel currents simulated under stationary conditions at pH show long-lived closed states interrupted by burst activity (Fig. 12 A, left); while those in response to pH jumps show a clear pH dependency of first latency. The presence of closed-state inactivation is well exemplified by the presence of null traces (Fig. 12 A, right). Analysis of the burst kinetics show that pH does not alter the closed and open duration within the burst, while voltage modulates the length of the burst as well as the duration of the closed and open events within it (Fig. 12 B). The model therefore fairly accurately recapitulates the burst behavior of KcsA in experimental measurements and represents a working scheme that frames the gating properties of KcsA in quantitative kinetic terms.

DISCUSSION

Mechanistic Interpretation of the Kinetic Scheme

In light of the extensive set of structural information now available for KcsA, our data provide a basis for mechanistic speculations on the conformational changes that govern various gating events in KcsA. At neutral pH, KcsA predominantly occupies a closed, nonconductive state, in which the bundle crossing at the intracellular mouth of the channel provides a formidable barrier to the passage of ions, thereby acting as a physical gate (stimulus-dependent activation gate or lower gate) (Roux et al., 2000). The high resolutions structure of KcsA most likely represents this closed state or one very close to it (Doyle et al., 1998; Zhou et al., 2001b). Protonation of the intracellular "binding sites" (possibly H25 residue, Takeuchi et al., 2007) causes hinge-based translations of TM2 (and to a small extent TM1) around the channel's central cavity, which is coupled to the opening of

the pore (Perozo et al., 1999). Akin to the mechanisms proposed for eukaryotic channels, the binding of protons and movements of individual TM segments might represent the set of independent subunit transitions (C_1-C_2-C_3-C_4), while the opening of the pore perhaps corresponds to a concerted pH-independent conformational change (C_5-O). Since the burst properties of KcsA are similar at different activating pH, ion conduction could be expected to progress only when all the subunits adopt a conductive conformation (as in C_5).

Multiple lines of evidences suggest that the open-conductive conformation of KcsA is intrinsically unstable (meta-stable state) (Cordero-Morales et al., 2006a). Once the proton-activated gate opens, the channel spontaneously transitions to a nonconductive, inactivated state with entry and exit rates modulated by membrane voltage (O-I_s). The inactivated state has been proposed to involve a constriction in the outer mouth of the filter with a possible loss of ion-binding sites (Liu et al., 1996; Kiss and Korn, 1998; Loots and Isacoff, 1998; Kiss et al., 1999). Although the molecular basis of the events that lead to inactivation are yet to be defined, the stability of the inactivated state in KcsA has been postulated to be governed by the interaction between residues Glu71 and Asp80 (Cordero-Morales et al., 2006a). While this interaction is seen in the high-resolution crystal structures of KcsA that represent the closed state of the channel, its role in inactivation seems to kick in only upon channel activation as would be expected if conformational changes associated with channel activation further strengthen this interaction. The steady-state single-channel properties of KcsA reveal the presence of two other short-lived nonconductive states (I_i and I_f) that the channel can visit before entering the long-lived inactivated state I_s. Since the occurrence and lifetimes of these states are modified by voltage but unaltered by pH, they might represent the short lived inactivated states arising from the dynamic nature of the selectivity filter. Transitions within the bursts are therefore defined by the $I_i \leftrightarrow O \leftrightarrow I_f$ equilibrium. Removal of the Glu71–Asp80 interaction in the E71A mutant dramatically destabilizes the I_s state, thereby the predominant transitions at steady state being $I_i \leftrightarrow O \leftrightarrow I_f$.

Inactivation requires at least partial activation of the channel, although full opening or ion conduction is not entirely mandatory (Chakrapani et al., 2007), thus suggesting that conformational changes associated with channel activation in some of the subunits are sufficient to trigger inactivation. Since channels seem to recover faster from these closed-inactivated states than from inactivated state originating from open conducting channel, these states might involve different extent of distortion of the filter. Recovery from inactivation or resetting of the filter back to its conductive conformation occurs upon closure of the lower gate, which in principle implies that a closed lower gate favors the conductive conformation of the filter while the open lower gate tends to facilitate a collapsed filter. Still, KcsA shows ~10% recovery under steady-state conditions. These recovering channels could represent a population that spontaneously recovers from inactivation (without closure of the lower gate) or, although less likely, could also denote channels in which the lower gate closes momentarily.

A thorough understanding of ion channel mechanics will eventually result from a combination of direct structural information with detailed functional characterization. Given the technical advances in the field of membrane protein crystallography and spectroscopy and the pace at which new high resolution structures of K^+ channels are being generated, we believe that this study provides an important framework to understand the mechanism of channel function.

We thank L. Cuello, V. Jogini, and F. Bezanilla for insightful discussions; and V. Vásquez, J. Santos, H. Raghuraman, and O. Dalmas for critical reading and comments on the manuscript.

This work was supported by National Institutes of Health grants to E. Perozo and an American Heart Association Postdoctoral Fellowship to S. Chakrapani.

Olaf S. Andersen served as editor.

Submitted: 13 June 2007
Accepted: 20 September 2007

REFERENCES

Aldrich, R.W., and C.F. Stevens. 1983. Inactivation of open and closed sodium channels determined separately. *Cold Spring Harb. Symp. Quant. Biol.* 48:147–153.

Aldrich, R.W., D.P. Corey, and C.F. Stevens. 1983. A reinterpretation of mammalian sodium channel gating based on single channel recording. *Nature.* 306:436–441.

Armstrong, C.M., and W.F. Gilly. 1979. Fast and slow steps in the activation of sodium channels. *J. Gen. Physiol.* 74:691–711.

Auerbach, A., and C.J. Lingle. 1986. Heterogeneous kinetic properties of acetylcholine receptor channels in *Xenopus* myocytes. *J. Physiol.* 378:119–140.

Ball, F.G., and M.S. Sansom. 1989. Ion-channel gating mechanisms: model identification and parameter estimation from single channel recordings. *Proc. R. Soc. Lond. B. Biol. Sci.* 236:385–416.

Bezanilla, F., and C.M. Armstrong. 1977. Inactivation of the sodium channel. I. Sodium current experiments. *J. Gen. Physiol.* 70:549–566.

Bezanilla, F., E. Perozo, D.M. Papazian, and E. Stefani. 1991. Molecular basis of gating charge immobilization in Shaker potassium channels. *Science.* 254:679–683.

Bezanilla, F., E. Perozo, and E. Stefani. 1994. Gating of Shaker K^+ channels. II. The components of gating currents and a model of channel activation. *Biophys. J.* 66:1011–1021.

Blunck, R., J.F. Cordero-Morales, L.G. Cuello, E. Perozo, and F. Bezanilla. 2006. Detection of the opening of the bundle crossing in KcsA with fluorescence lifetime spectroscopy reveals the existence of two gates for ion conduction. *J. Gen. Physiol.* 128:569–581.

Chakrapani, S., J.F. Cordero-Morales, and E. Perozo. 2007. A quantitative description of KcsA gating I: macroscopic currents. *J. Gen. Physiol.* 130:465–478.

Chapman, M.L., and A.M. VanDongen. 2005. K channel subconductance levels result from heteromeric pore conformations. *J. Gen. Physiol.* 126:87–103.

Chapman, M.L., H.M. VanDongen, and A.M. VanDongen. 1997. Activation-dependent subconductance levels in the drk1 K channel suggest a subunit basis for ion permeation and gating. *Biophys. J.* 72:708–719.

Colquhoun, D., and A.G. Hawkes. 1982. On the stochastic properties of bursts of single ion channel openings and of clusters of bursts. *Philos. Trans. R. Soc. Lond. B Biol. Sci.* 300:1–59.

Cordero-Morales, J.F., L.G. Cuello, Y. Zhao, V. Jogini, D.M. Cortes, B. Roux, and E. Perozo. 2006a. Molecular determinants of gating at the potassium-channel selectivity filter. *Nat. Struct. Mol. Biol.* 13:311–318.

Cordero-Morales, J.F., L.G. Cuello, and E. Perozo. 2006b. Voltage-dependent gating at the KcsA selectivity filter. *Nat. Struct. Mol. Biol.* 13:319–322.

Cortes, D.M., and E. Perozo. 1997. Structural dynamics of the *Streptomyces lividans* K^+ channel (SKC1): oligomeric stoichiometry and stability. *Biochemistry.* 36:10343–10352.

Cuello, L.G., J.G. Romero, D.M. Cortes, and E. Perozo. 1998. pH-dependent gating in the *Streptomyces lividans* K^+ channel. *Biochemistry.* 37:3229–3236.

Delcour, A., H.D. Lipscombe, and R.W. Tsien. 1993. Multiple modes of N-type calcium channel activity distinguished by differences in gating kinetics. *J. Neurosci.* 13:181–194.

Doyle, D.A., J. Morais Cabral, R.A. Pfuetzner, A. Kuo, J.M. Gulbis, S.L. Cohen, B.T. Chait, and R. MacKinnon. 1998. The structure of the potassium channel: molecular basis of K^+ conduction and selectivity. *Science.* 280:69–77.

Dreyer, I., E. Michard, B. Lacombe, and J.B. Thibaud. 2001. A plant *Shaker*-like K^+ channel switches between two distinct gating modes resulting in either inward-rectifying or "leak" current. *FEBS Lett.* 505:233–239.

Goldman, L., and J.L. Kenyon. 1982. Delays in inactivation development and activation kinetics in myxicola giant axons. *J. Gen. Physiol.* 80:83–102.

Goldman, L., and C.L. Schauf. 1972. Inactivation of the sodium current in Myxicola giant axons. Evidence for coupling to the activation process. *J. Gen. Physiol.* 59:659–675.

Gross, A., L. Columbus, K. Hideg, C. Altenbach, and W.L. Hubbell. 1999. Structure of the KcsA potassium channel from *Streptomyces lividans*: a site-directed spin labeling study of the second transmembrane segment. *Biochemistry.* 38:10324– 10335.

Heginbotham, L., M. LeMasurier, L. Kolmakova-Partensky, and C. Miller. 1999. Single streptomyces lividans K^+ channels: functional asymmetries and sidedness of proton activation. *J. Gen. Physiol.* 114:551–560.

Hess, P., J.B. Lansman, and R.W. Tsien. 1984. Different modes of Ca channel gating behaviour favoured by dihydropyridine Ca agonists and antagonists. *Nature.* 311:538–544.

Hodgkin, A.L., and A.F. Huxley. 1952. A quantitative description of membrane current and its application to conduction and excitation in nerve. *J. Physiol.* 117:500–544.

Horn, R., and K. Lange. 1983. Estimating kinetic constants from single channel data. *Biophys. J.* 43:207–223.

Hoshi, T., W.N. Zagotta, and R.W. Aldrich. 1994. Shaker potassium channel gating. I: transitions near the open state. *J. Gen. Physiol.* 103:249–278.

Jackson, M.B., B.S. Wong, C.E. Morris, H. Lecar, and C.N. Christian. 1983. Successive openings of the same acetylcholine receptor channel are correlated in open time. *Biophys. J.* 42:109–114.

Jiang, Y., A. Lee, J. Chen, M. Cadene, B.T. Chait, and R. MacKinnon. 2002. The open pore conformation of potassium channels. *Nature.* 417:523–526.

Kelly, B.L., and A. Gross. 2003. Potassium channel gating observed with site-directed mass tagging. *Nat. Struct. Biol.* 10:280–284.

Kiss, L., and S.J. Korn. 1998. Modulation of C-type inactivation by K^+ at the potassium channel selectivity filter. *Biophys. J.* 74:1840–1849.

Kiss, L., J. LoTurco, and S.J. Korn. 1999. Contribution of the selectivity filter to inactivation in potassium channels. *Biophys. J.* 76:253–263.

Kuo, C.C., and B.P. Bean. 1994. Na^+ channels must deactivate to recover from inactivation. *Neuron.* 12:819–829.

LeMasurier, M., L. Heginbotham, and C. Miller. 2001. KcsA: it's a potassium channel. *J. Gen. Physiol.* 118:303–314.

Liu, Y., M.E. Jurman, and G. Yellen. 1996. Dynamic rearrangement of the outer mouth of a K^+ channel during gating. *Neuron.* 16:859–867.

Liu, Y., S.P. Sompornpisut, and E. Perozo. 2001. Structure of the KcsA channel intracellular gate in the open state. *Nat. Struct. Biol.* 8:883–887.

Loots, E., and E.Y. Isacoff. 1998. Protein rearrangements underlying slow inactivation of the *Shaker* K^+ channel. *J. Gen. Physiol.* 112:377–389.

MacKinnon, R. 1991. Determination of the subunit stoichiometry of a voltage-activated potassium channel. *Nature.* 350:232–235.

McCormack, K., W.J. Joiner, and S.H. Heinemann. 1994. A characterization of the activating structural rearrangements in voltage-dependent *Shaker* K^+ channels. *Neuron.* 12:301–315.

Meuser, D., H. Splitt, R. Wagner, and H. Schrempf. 1999. Exploring the open pore of the potassium channel from *Streptomyces lividans*. *FEBS Lett.* 462:447–452.

Milescu, L.S., G. Akk, and F. Sachs. 2005. Maximum likelihood estimation of ion channel kinetics from macroscopic currents. *Biophys. J.* 88:2494–2515.

Milone, M., H.L. Wang, K. Ohno, R. Prince, T. Fukudome, X.M. Shen, J.M. Brengman, R.C. Griggs, S.M. Sine, and A.G. Engel. 1998. Mode switching kinetics produced by a naturally occurring mutation in the cytoplasmic loop of the human acetylcholine receptor epsilon subunit. *Neuron.* 20:575–588.

Naranjo, D., and P. Brehm. 1993. Modal shifts in acetylcholine receptor channel gating confer subunit-dependent desensitization. *Science.* 260:1811–1814.

Oxford, G.S. 1981. Some kinetic and steady-state properties of sodium channels after removal of inactivation. *J. Gen. Physiol.* 77:1–22.

Papazian, D.M., L.C. Timpe, Y.N. Jan, and L.Y. Jan. 1991. Alteration of voltage-dependence of *Shaker* potassium channel by mutations in the S4 sequence. *Nature.* 349:305–310.

Patlak, J.B., M. Ortiz, and R. Horn. 1986. Opentime heterogeneity during bursting of sodium channels in frog skeletal muscle. *Biophys. J.* 49:773–777.

Perozo, E., D.M. Cortes, and L.G. Cuello. 1998. Three-dimensional architecture and gating mechanism of a K^+ channel studied by EPR spectroscopy. *Nat. Struct. Biol.* 5:459–469.

Perozo, E., D.M. Cortes, and L.G. Cuello. 1999. Structural rearrangements underlying K^+-channel activation gating. *Science.* 285:73–78.

Qin, F., A. Auerbach, and F. Sachs. 1996. Estimating single-channel kinetic parameters from idealized patch-clamp data containing missed events. *Biophys. J.* 70:264–280.

Qin, F., A. Auerbach, and F. Sachs. 1997. Maximum likelihood estimation of aggregated Markov processes. *Proc. Biol. Sci.* 264:375–383.

Roux, B., and R. Sauve. 1985. A general solution to the time interval omission problem applied to single channel analysis. *Biophys. J.* 48:149–158.

Roux, B., S. Berneche, and W. Im. 2000. Ion channels, permeation, and electrostatics: insight into the function of KcsA. *Biochemistry.* 39:13295–13306.

Schoppa, N.E., and F.J. Sigworth. 1998a. Activation of *Shaker* potassium channels. I. Characterization of voltage-dependent transitions. *J. Gen. Physiol.* 111:271–294.

Schoppa, N.E., and F.J. Sigworth. 1998b. Activation of *Shaker* potassium channels. III. An activation gating model for wild-type and V2 mutant channels. *J. Gen. Physiol.* 111:313–342.

Schrempf, H., O. Schmidt, R. Kummerlen, S. Hinnah, D. Muller, M. Betzler, T. Steinkamp, and R. Wagner. 1995. A prokaryotic potassium ion channel with two predicted transmembrane segments from *Streptomyces lividans*. *EMBO J.* 14:5170–5178.

Sigworth, F.J., and S.M. Sine. 1987. Data transformations for improved display and fitting of single-channel dwell time histograms. *Biophys. J.* 52:1047–1054.

Smith-Maxwell, C.J., J.L. Ledwell, and R.W. Aldrich. 1998. Role of the S4 in cooperativity of voltage-dependent potassium channel activation. *J. Gen. Physiol.* 111:399–420.

Splitt, H., D. Meuser, I. Borovok, M. Betzler, and H. Schrempf. 2000. Pore mutations affecting tetrameric assembly and functioning of the potassium channel KcsA from *Streptomyces lividans*. *FEBS Lett.* 472:83–87.

Stuhmer, W. 1992. Electrophysiological recording from *Xenopus* oocytes. *Methods Enzymol.* 207:319–339.

Takeuchi, K., H. Takahashi, S. Kawano, and I. Shimada. 2007. Identification and characterization of the slowly exchanging pH-dependent conformational rearrangement in KcsA. *J. Biol. Chem.* 282:15179–15186.

Tytgat, J., and P. Hess. 1992. Evidence for cooperative interactions in potassium channel gating. *Nature.* 359:420–423.

Vandenberg, C.A., and F. Bezanilla. 1991. A sodium channel gating model based on single channel, macroscopic ionic, and gating currents in the squid giant axon. *Biophys. J.* 60:1511–1533.

Wyllie, D.J., P. Behe, and D. Colquhoun. 1998. Single-channel activations and concentration jumps: comparison of recombinant NR1a/NR2A and NR1a/NR2D NMDA receptors. *J. Physiol.* 510(Pt 1):1–18.

Zagotta, W.N., T. Hoshi, and R.W. Aldrich. 1994. *Shaker* potassium channel gating. III: Evaluation of kinetic models for activation. *J. Gen. Physiol.* 103:321–362.

Zhou, M., J.H. Morais-Cabral, S. Mann, and R. MacKinnon. 2001a. Potassium channel receptor site for the inactivation gate and quaternary amine inhibitors. *Nature.* 411:657–661.

Zhou, Y., and R. MacKinnon. 2003. The occupancy of ions in the K^+ selectivity filter: charge balance and coupling of ion binding to a protein conformational change underlie high conduction rates. *J. Mol. Biol.* 333:965–975.

Zhou, Y., J.H. Morais-Cabral, A. Kaufman, and R. MacKinnon. 2001b. Chemistry of ion coordination and hydration revealed by a K^+ channel-Fab complex at 2.0 Å resolution. *Nature.* 414:43–48.